DEPENDENCE OF STRUCTURAL AND OPTICAL PROPERTIES OF THE TERNARY SEMICONDUCTORS ON PREPARATION TECHNIQUES

Abstract

Ternary compounds are widely used in the fabrication of solar cells. The optical properties of pure and doped ZnS, CdZnS and PbZnS semiconductor compounds are reviewed based on synthesis mechanisms and various dopants. The nature of dopants, the incurred structural modifications and change in energy bandgap are reasoned. The effect of synthesis mechanism and annealing temperature on grain size, that further controls the optical properties, are explained. Although co-precipitation method is predominantly used by most of the researchers because of its energy efficiency, simple and quick preparation method, ease of handling particle size, other important synthesis mechanisms like co-precipitation method, solid-state reaction method and solvothermal methods are also discussed elaborately. Various collected nanoparticles data reveals that the bandgap varies from 2eV to 4.5eV and higher bandgap materials are preferred for window materials in solar cell applications.

Key words: Solar cell; Ternary Semiconductor; Energy gap; Electro-negativity.

Authors

G. Ganesh
Department of Physics and Nanotechnology,
SRM Institute of Science and Technology,
Kattankulthur, Chennai- 603 203, India.

N. Pavan Kumar
Department of Sciences and Humanities,
Matrusri Engineering College,
Saidabad, Hyderabad – 500 059, India.

T. Shekharam
Department of Sciences and Humanities,
Matrusri Engineering College,
Saidabad, Hyderabad – 500 059, India.

P. Gayathri Pavani
Department of Freshman Engineering,
Sphoorthy Engineering College,
Nadargul, Hyderabad-501510, India.

Y. Anantha Lakshmi
Department of Science and Humanities,
MLR Institute of Technology,
Hyderabad-500 043, India.

Y. Vasudeva Reddy
Department of Physics,
Government City College,
Nayapul, Hyderabad – 500 002, India.
yvasudevreddy@yahoo.com

I. INTRODUCTION

According to the second law of thermodynamics, the available energy of the universe decreases continuously, so it is essential to focus on non-conventional energy sources. The best alternative for normal energy is solar energy, because of its abundant availability throughout the globe. The main challenge is how to convert this solar energy into useful energy. For this purpose, researchers put their focus on the materials, which effectively change solar energy into conventional energy. The solar cell is the device that converts solar energy into electrical energy. Solar cells or photovoltaic (PV) cells work on the principle of the photoelectric effect, in which, the photons hit the surface of the target element and the energy of the incident photons are completely transferred to the electrons present in the valence band of the element. This energy is sufficient to stimulate the electrons to the conduction band and henceforth it gives rise to ejection of free electrons. These free electrons are responsible for the electric current in the circuit. The element on which the photons strike can be either a semiconducting or conducting material. In insulators, the energy band gap between the valence band and conduction band is very large (usually greater than 6 eV). Generally, the photons from the sunlight do not possess this amount of energy to stimulate the electrons from the valence to conduction band for such insulators. Whereas, in conductors, these bands almost overlap with each other and hence a greater number of free electrons can be made available using solar energy photons. These free electrons alone cannot establish current unless they are forced to move in one direction in the circuit, which thus requires an external electric field. However, in case of semiconductors, the gap between the valance band and conduction band is less than those of insulators which photons of UV/visible spectrum can do the task of exciting the electrons. Further, due to the presence of a pn-junction, there is a small electric field present within the semiconductors due to the partial recombination of electrons and holes, which acts as a driving force for the free electrons, that is the reason why semiconductors are used in PV cells.

An ideal solar cell has a band gap value of 1.4 eV to absorb the maximum number of photons from the solar radiation [1]. The energy of photons in the solar spectrum ranges from 3.54 eV to 1.45 eV. So, while designing the solar cell, two factors are crucially considered: the absorption of as many photons as from the incident radiation and the minimization of material cost. Binary semiconductors are economically cheaper, but the main limitation of such materials is its discrete energy gap. Whereas, ternary compounds, which are though relatively costlier, tailoring of band gap energy is possible with [2-5]. For this reason, ternary compounds are widely used in the making of solar cells and photovoltaic devices. The widely used ternary semiconductor materials are Cadmium Zinc Sulfide (CdZnS) and Lead Zinc Sulfide (PbZnS) [6-16]. ZnS shows enormous optical transparency in the whole spectral range from UV to IR [17]. It is an environment-friendly, low priced, thermally and synthetically stable material [18], but the major limitation is its poor electrical conductivity. For this purpose ZnS is mixed with either CdS or PbS to enhance its electrical conductivity. Improvement in electrical and optical properties can also be obtained by doping CdZnS and PbZnS with Sm, Na, Cu, Mg metal ions [19-24]. Doping with different ionic radii metal ions results in structural modification which is responsible for the observed changes in the optical and other transport properties. In addition to doping, synthesis mechanism and annealing temperature also play significant roles in the modification of optical and other properties. Moreover, annealing temperature also affects the grain size, which leads to notable change in band. Considering all these above facts, the objective of this paper is to review the optical properties in connection with structural modifications of pure and doped CdZnS and PbZnS ternary semiconductor compounds, synthesized using different synthesis mechanisms and various dopants.

II. SYNTHESIS METHODS

Ternary semiconductor compounds can be prepared through several methods such as the Co-precipitation method, solid-state reaction method, solve thermal method etc. Each of these methods has its own advantages and disadvantages. Moreover, the method of preparation affects the structural and morphological aspects of the compounds that modifies the optical properties of the compounds. Here, some of these methods are described with their important features, advantages and limitations.

1. **Co-Precipitation Method:** In this method, the starting materials are usually nitrates/acetates/sulfides/oxides of the elements, which dissolve easily in water and get mixed well, producing a homogeneousness solution. The Co-precipitation (CP) method is simple, takes less time and easy in terms of controlling the particle size and compositions. It has several ways to adjust the surface and homogeneous state of the solution and does not need any carbon-based solvents. The only drawback of this method is the management of its toxic unused liquid waste during the synthesis process.

   In synthesis of ZnS and Pb-doped ZnS compounds through the CP method [25-26], initially, all the Lead acetate, Zinc acetate, iron, Thiourea sodium sulfide and citric acid were mixed in stoichiometric composition and dissolved in deionized water to make 1M solutions. The solution mixture kept under a continuous stirring process. The solution of Triethanolamine (TEA), a complexing mediator is added to the solution mixture. After few minutes, Ammonium hydroxide is added under constant stirring to keep the pH value 10. The solution is heated at 70 ºC with constant stirring until the color of the solution turns grey precipitation. The formed precipitate is further heated for 3h. The dried precipitate is calcined for 2h at 300 °C in nitrogen atmosphere in a furnace. To obtain a uniform particle size, the dried precipitate is ground well into powder.

2. **Solid State Reaction Method:** The solid-state reaction method is the mostly used synthesis method for the preparation of the single crystalline and polycrystalline compounds. It is a low-cost method; easy process and it is an appropriate method for the large-scale production in industries. This method requires high temperature as compared to other chemical methods which is the limitation of this method [27]. For the synthesis of ZnS and Ni (0.5–2.0 at. %) doped solution mixtures by solid state reaction method, the starting materials used are, $Zn(CH_3COO)_2.2H_2O$, $NiCl_2$ and thiourea, which are taken in a mortar and are ground thoroughly, along with acetone mixing for every 30 minutes to get a homogeneous mixture. After which, the compounds are calcined for 4 hours at 400 °C in nitrogen atmosphere in a furnace. The calcined powder is then washed with de-ionized water for many times to remove impurities and dried in a hot air oven at 100 ºC.

3. **Solvothermal Method:** Solvothermal method is used for preparing a variety of materials such as conductors, semiconductors, ceramics, and polymers. The process involves the use of a solvent under moderate to high pressure (typically between 1 atm and 10,000 atm) and temperature (typically between 100 °C and 1000 °C) that facilitates the

interaction of precursors during synthesis [28]. ZnS has been prepared by using precursors such as, zinc chloride, ethylene glycol and thiourea, dissolved in a distilled water under constant stirring. After few minutes polyvinylpyrrolidone (PVP) is added to it while stirring the solution continuously. The final mixture is transferred to an autoclave and calcined at 200° C for 5 hours in a furnace. After centrifuging the precipitate at a high speed of 12,000 rpm, it is washed with de-ionized water and ethanol. Then the precipitate is dried in a hot air oven at 100 ºC and grounded to form fine powder.

Co-precipitation (CP), solid state and solvothermal are some of the methods used for ZnS and CdS nanoparticles, out of which CP method is predominantly used by most of the researchers, because of its energy efficiency, several possibilities to change the particle surface and overall homogeneity. In addition to these, its simple and quick preparation technique and ease of control of particle size, are some major factors which favour the use of co-precipitation method over other methods.

III. STRUCTURAL CHARACTERIZATION

Research on different synthesis techniques, different temperature treatments, and different doping methods to eliminate secondary phases and to produce better structural transformations in ternary semiconducting compounds have been noteworthy. Some of those results have been reviewed in the subsequent paragraphs.

The pure ZnS compound, prepared by CP method [26], has shown a hexagonal structure with lattice constants, 3.86A° and 6.24A°. The Pb-doped ZnS with the compositional formula $Zn_{1-x}Pb_xS$ (x= 0 to 0.4), synthesized by CP method [26] and sintered at 800˚C for 2 hours rapidly have also retained hexagonal structure. XRD pattern confirms the formation of the single-phase structure, no secondary peaks are seen as observed from figure-1 which confirms Pb^{2+} ions are well substituted in the ZnS lattice. With the increase in the concentration of Pb in ZnS, lattice parameters has increased due to the ionic radius inequality between Pb^{2+}(1.19A°) and Zn^{2+} (0.72A°). Similar compounds prepared through solid state method have also produced similar results.

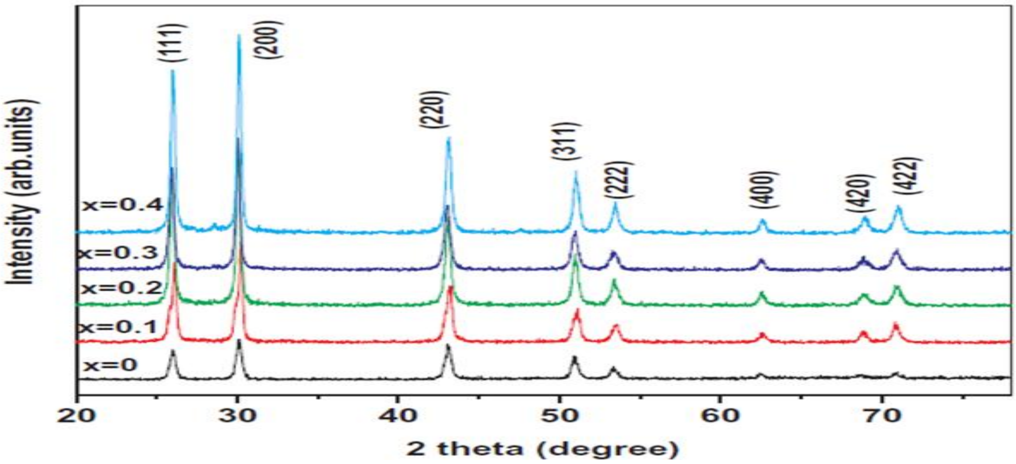

Figure1: XRD patterns of Pb-ZnS samples (taken from Ref.26)

$Pb_{1-x}Zn_xS$ (x=0, 0.1, 0.2, 0.3, 0.4) samples, synthesized by CP method, have shown cubic symmetry in its crystal structure. Increase in the lattice parameters is seen with Zn concentration which could be due to the occupancy of some Zn ions in the interstitial positions of the lattice. Lattice constants are monotonically increasing from 5.92 Å, 5.93 Å, 5.94 Å, and 5.95 Å for the respective dopant concentrations, i.e. x=0.1 to 0.5. The crystallite size is found to be decreasing with increase in Zn concentration as reported by Vasudeva Reddy et.al [15]. The semiconductor compounds of $Cd_{0.8}Zn_{0.2}S$ doped with Sm^{3+} (0.01, 0.02, 0.03, 0.04, & 0.05) samples, prepared by CP method, exhibit polycrystalline hexagonal phase. No diffraction peaks in the XRD pattern has shown correspondence to any impurity phase [22]. Al doped ZnS ($Zn_{1-x}Al_xS$) nanoparticles with different Al concentrations (x=0.00, 0.02, 0.04, 0.06, 0.08 and 0.10), synthesized by CP method, confirm cubic structure without any secondary peaks. Lattice parameters decrease with doping because of the higher ionic radii of Zn^{2+} (0.74 Å) as compared to Al^{3+} (0.51 Å). The lattice parameter (a) of x=0.00, 0.02, 0.04, 0.06, 0.08 and 0.10 are found to be 6.109, 6.098, 6.092, 6.069, 6.062 and 6.054 Å respectively [29]. In Fe^{2+}, Co^{2+}, Ni^{2+} doped ZnS compounds [30], synthesized by solvothermal method with low dopant concentrations (1%), employing polyvinyl pyrrolidone (PVP) as a capping agent, the structure is found to be of cubic symmetry at room temperature. With doping the structure of nanoparticles remains to be cubic but the size of nanoparticle is reduced.

In Ni-doped ZnS samples, the lattice parameters are observed to be decreasing with increase in Ni concentration because the ionic radius of Ni (0.69 Å) is less than that of Zn (0.74 Å) [31]. The Li^{3+} and Nd^{3+} co-doping on structure of L-arginine-passivated ZnS nanoparticle, synthesized by chemical CP method, the XRD results of nanoparticles show the hexagonal structure with particle size 4.6 -1.8 nm with an average size of 3 nm and HR-TEM confirms the same. The size of nano particle of ZnS reduces as the co-dopant concentration increases, any diffraction peaks of co-dopant Nd^{3+} are not found, then the line width is broadened due to loss of long-range order relative to the bulk. The width of peaks also broadens due to lattice strain [32]. For co-doped ZnS compound $Zn_{1-x}Co_xS$ (x=0, 0.1, 0.2, 0.3), synthesized by the CP method, its XRD pattern shows a single phase cubic structure and complete solubility of Co in ZnS is observed. The ionic radii of $Co^{2+}$and $Zn^{2+}$are 0.72 Å and 0.74 Å respectively [33]. The similar compound, cobalt (0, 1, 5, and 10 %)-doped ZnS nanoparticles, prepared through solvothermal method also shows cubic phase. While undoped ZnS has lattice constant, 5.38 Å, co-doped ZnS of (1%,5% and 10%) have lattice constants 5.36 Å,5.34 Å and 5.31 Å respectively. The decrease in the lattice parameters may be ascribed to strain induced in ZnS lattice with insertion of Co ions [28].

Similarly, Cr-doped ZnS compound $Zn_{1-x}Cr_xS$ (x=0.00, 0.01, 0.03, 0.05, 0.07) nanoparticles are synthesized by CP method using thioglycerol as the caping agent. XRD pattern identifies a Zinc blende structure with no secondary phase, indicating that Cr ion has replaced Zn in the ZnS. Decrease in lattice parameter is due to the ionic radius of Cr (0.63 Å) which is less than the ionic radius of Zn (0.74 Å) [34]. From another study, Cr -doped $Zn_{1-x}Cr_xS$ nanoparticles with x = 0.00, 0.005, 0.01, 0.02 and 0.03, synthesized by CP method, has shown cubic structure. The average crystallite size decreases with the increase of Cr concentration and lies in the range 6-10 nm. The lattice parameters of $Zn_{1-x}Cr_xS$ nano powders, obtained from the XRD data, appear to be decreasing in a narrow range 5.4−5.2 Å with increasing Cr content [35]. The XRD pattern of the pure CdS nanoparticles, synthesized by CP method, revealed single phase and hexagonal structure. Lattice Parameters are a= 4.143 Å, c= 6.719 Å [36].

L S Devi et al studied the Mn-doped CdS (X=0, 0.02, 0.04, 0.06, 0.08, 0.1) compound, synthesized by CP method, showed cubic structure. The lattice parameters are found to be 5.729 Å, 5.723 Å, 5.717 Å, 5.721 Å, 5.693 Å and 5.726 Å for the 0, 2, 4, 6, 8 and 10 % doped samples respectively. The evaluated crystallite size of CdS nano particles doped with different concentrations of Mn^{2+} is in the range of 3.3–2.3 nm [37]. Thambidurai et al observed the Cr-doped CdS nanoparticles, synthesized by CP method, whose X-ray diffraction analysis revealed hexagonal structure of the samples. The average particle size of the nanoparticles is obtained in the range of 2.2-3.8 nm. The doping of Cr in CdS does not lead to any structural phase transformation but the lattice constant values are found to be decreasing and it is due to the ionic radii of Cr (0.63 Å) which is less than that of Cd^{2+} (0.96 Å) [38].

In the study of $Cd_{0.8-X}Pb_xZn_{0.2}S$ semiconductor compound, synthesized by CP method, the XRD results revealed that both cubic and hexagonal phases are present in the compound. Hexagonal only peaks are observed in the compound $Cd_{0.8-X}Pb_xZn_{0.2}S$ with x = 0, whereas, both hexagonal and cubic phases are present in the mixed crystals with x = (0.1 - 0.6) and only peaks corresponding to cubic phases are seen in the samples with x = 0.7 and 0.8. Overall, the $Cd_{0.8-X}Pb_xZn_{0.2}S$ compounds undergo a crystalline transition from hexagonal to cubic i.e., the structure changes from lower symmetry to higher symmetry. Hexagonal structure of $Cd_{0.8-X}Pb_xZn_{0.2}S$ compound is due to major peaks occurring from the reflections of (100), (002), (101), the average crystalline size in $Cd_{0.8-X}Pb_xZn_{0.2}S$ compounds decreases with the increase in Pb content, face centred cubic structure of PbS is assigned with the major peaks from the planes (111), (200) [39]. G. Yellaiah et al [20] observed the Sm doped $Cd_{0\cdot8}Zn_{0\cdot2}S$ compound with different amounts of samarium (0.01, 0.02, 0.03, 0.04 and 0.05 M), synthesized by the CP method where the XRD pattern showed a single phase with hexagonal structure. The average crystallite size of the compound is found in the range of 40 –90 nm. G. Yellaiah et al [19] studied the Na doped $Cd_{0\cdot8}Zn_{0\cdot2}S$ compound with different amounts of samarium (0.00, 0.03, 0.1, 0.2 and 0.3), synthesized by the CP method, revealed single phase hexagonal structure. The average crystallite size of the compound was found between 29 and 55 nm.

The discussed structural results in correspondence to the synthesis methods, are tabulated in table 1.

Table 1: Different synthesizing methods used to prepare various compounds and their structures

S. No	Compound	Synthesis method	Heating conditions	structure
1	$Zn_{1-X}Pb_XS$ [26]	Co-precipitation method	Calcined at 2 h at 300 ˚C / sintered at 800˚C for 2 h	Hexagonal
2	$Zn_{1-X}Cr_XS$ [35]	Co-precipitation method	In oven for 50 ˚C for 4 h	Cubic
3	Al doped ZnS [29]	Co-precipitation method	In oven for 6 h at 60 ˚C	Cubic
4	(Fe, Ni, Co) doped ZnS [30]	Solvothermal method	Heated in furnace at 200 ˚C for 5 h	Cubic
5	Mn doped CdS [37]	Co-precipitation method	Dried at 60 ˚C for 24 h	Cubic
6	Cr doped ZnS [34]	Co-precipitation method	Dried at 60 ˚C for overnight	Cubic
7	Li, Nd doped ZnS [32]	Co-precipitation method	Dried at 40 ˚C for 16 h	Hexagonal
8	Cr doped CdS [38]	Co-precipitation method	Dried at 100 ˚C for 4 h	Hexagonal
9	$Pb_{1-x}Zn_xS$ [15]	Co-precipitation method	Calcined sm0˚C for 2h /sintered at 800˚C for 2 h	Cubic
10	Sm doped $Cd_{0.8}Zn_{0.2}S$ [22]	Co-precipitation method	Calcined 300 ˚C for 2h /sintered at 800 ˚C for 2 h	Hexagonal
11	Ni doped ZnS [27]	solid state method	Calcined at 400 °C for 4 h	Cubic
12	Co doped ZnS [33]	Solvothermal	Heated 180˚C for 10 hours	Cubic
13	CdS [36]	Co-precipitation method	Heated at 300 °C for 2h	Hexagonal
14	Sm doped $Cd_{0\cdot8}Zn_{0\cdot2}S$ [20]	Co-precipitation method	Calcined 300 ˚C for 2h /sintered at 800 ˚C for 2 h	Hexagonal

15	Na doped $Cd_{0\cdot8}Zn_{0\cdot2}S$ [19]	Co-precipitation method	Calcined 300 ˚C for 2h /sintered at 800 ˚C for 2 h	Hexagonal
16	Co doped ZnS (28)	Co-precipitation method	Calcined 300 ˚C for 2h in vacuum	Cubic

IV. OPTICAL PROPERTIES

The band gap value of pure ZnS compound prepared by CP method, studied by the Vasudeva Reddy et al [26], is 3.6 eV. When it is doped with Pb, the energy gap values change from 3.6 eV to 2.9 eV. As the Pb concentration increases, the energy gap values decrease, because the binding force of Pb is less as compared to that of Zn i.e. the energy needs to break the bond is lesser in case of Pb than for Zn.

T. Shekharam et al have studied the optical properties of $Cd_{0.8-x}Pb_xZn_{0.2}S$ compounds (x = 0, 0.1, 0.4, 0.6, 0.7, 0.8) which are synthesized by CP method. The optical absorption of $Cd_{0.8-x}Pb_xZn_{0.2}S$ compounds falls in the wavelength region, 496–508 nm. The energy gap varying from 2.55- 4.43 eV, indicates that as the Pb concentration increases, the band gap values increase [39]. D. Amaranatha Reddy et al [40] studied $Zn_{1-x}Cr_xS$ (x = 0.00, 0.005, 0.01, 0.02 and 0.03) compounds, show band-gap values varying from 3.81eV to 4.03 eV. Energy gap values increase with the increase in Cr concentration. The band gap of pure and Cr-ZnS nano particles show an increase in band gap when compared to bulk ZnS (3.6 eV). The particle size decreases in Cr-ZnS and the absorption peak shifts to lower wavelength indicating doped Cr-ZnS forms a new energy level in the band structure of ZnS. From Namrata Dixit et al studied optical properties of Ni^{+2} -ZnS compounds, synthesized by CP method, it is found that as the Ni doping concentration increases, band gap values decrease from 4.43 eV (pure) to 4.29 eV (Ni-ZnS). The synthesized nanoparticles show an increase in band gap when compared with bulk ZnS (3.68eV). The Ni^{2+} doped samples show absorption spectrum between 285 and 290 nm and that of undoped ZnS, show at 280 nm. The intensity of absorption decreases as well with the increase in dopant concentration [41].

D.Amaranatha Reddy et.al studied various ZnS base compounds such as ZnS, $Zn_{0.97}Mn_{0.03}S$, $Zn_{0.97}Cr_{0.03}S$ and $Zn_{0.94}Mn_{0.03}Cr_{0.03}S$ nanoparticles. These compounds were synthesized by CP method. ZnS nanoparticles exhibited optical absorption edge around 326 nm, a marked blue shift compared to the bulk (338nm), which was believed to be caused by the quantum size effect as the size of nanoparticles fell into atomic scale. The absorption maxima for samples doped with Mn, Cr and co-doped with Mn and Cr appeared at 313, 308 and 303 nm respectively. The corresponding band gap value was found to be 3.81 eV. The energy gap values corresponding to these maxima were, 3.97, 4.03 and 4.09 eV respectively [42]. D. Amaranatha Reddy et.al [29] studied the energy bandgap of Al-ZnS compounds which were synthesized by CP method. The observed bandgap values of nano particles were in the range of 3.73-4.01 eV, a slightly higher than that of bulk ZnS (3.7 eV). The DRS studies reveal that the bandgap increased with increasing Al concentration. Observed blue shift was attributed to quantum confinement effects because of the 3-5nm sized nanoparticles which decreased with the increase in Al content showing a size dependent blue shift phenomenon of DRS edge.

The transition metal (Fe^{2+}, Co^{2+}, Ni^{2+}) – ZnS compounds were synthesized by solvothermal method. The optical properties of these materials were studied by Z. Dehghani et al [30]. The energy bandgap values varied from 3.92 to 3.49 eV. The UV-Visible spectroscopy exhibited the absorption edge shift towards lower wavelength with doping Fe, Ni, Co. Similarly, Devadoss et al studied the optical properties of Cu doped $Cd_{0.9}Zn_{0.1}S$ compounds which were synthesized by ?? method. The Cu doping $Cd_{0.9}Zn_{0.1}$ position of absorption edge shifted towards lower wavelength side (the blue shift) when doping of Cu is increased from 0% to 2%. The observed absorption shift towards lower side was an indication of the proper substitution of Cu^{2+} into the Cd^{2+} ions conforming the quantum confinement effect [43]. The optical absorption spectra of undoped and Ni-doped ZnS were studied by R. Sanjeev Kumar et al [31]. The absorption edge was found around 320–340 nm, a blue shift to that of bulk ZnS (345 nm) attributing to quantum size confinement. The measured bandgap of the undoped ZnS was 3.82 eV, for 3.3% Ni-doped ZnS, 3.70 eV and for 5.36% Ni-doped ZnS, 3.67 eV. It is observed that the band gap decreased with increasing Ni concentration. The photoluminescence spectra showed that the intensity of photoluminescence emission also decreased with increase in Ni concentration.

The optical properties of Sm doped $Cd_{0\cdot8}Zn_{0\cdot2}S$ nano crystals, synthesized by CP method has been studied by G. Yellaiah [20]. The bandgap values vary from 3.18 – 2.52 eV, showing a decrease with increasing Sm concentration. G. Yellaiah et al have also studied the optical properties of Na doped $Cd_{0\cdot8}Zn_{0\cdot2}S$ nano crystals, synthesized by CP method. The energy bandgap of undoped $Cd_{0.8}Zn_{0.2}S$ is 2.58 eV and that of Na doped, energy gap increases from 2.58 to 3.18 eV with the increasing dopant (Na) concentration [19]. The optical absorption of Cu doped ZnS, prepared by CP method, studied by V. Laxminarasimha Rao et al [44], show bandgap values, ranging between 3.92 – 3.51 eV. The decrease in bandgap with increase in copper concentration is attributed to the effect on the atomic distance and grain size. V. Laxminarasimha Rao et al have also studied the optical properties of Co doped ZnS ($x=0$, 0.02, 0.04, 0.06, 0.08, 0.1) compounds, prepared by CP method, for which the bandgap values fall between 3.91 to 3.62 eV, monotonically decreasing with increase in cobalt concentration. The decrease in band gap with cobalt concentration can be attributed to the change in band strength between ZnS and CoS as well as to the change in atomic distances and grain size. For low concentrations of cobalt, optical band gap of the material, change from 3.91 to 3.62 eV [45]. Also from Sambasivam et al [33] report on the Co-doped ZnS compound $Zn_{1-x}Co_xS$ ($X=0$, 0.1, 0.2, 0.3), synthesized by the CP method, the energy bandgap values are found varying from 3.78 – 3.93 eV, indicating the increase in the band gap with increase of cobalt concentration. Some such studies on the optical properties are presented in table 2.

Table 2: Compounds with the Energy gaps suitable for window materials in solar applications

S. No	**Name of the Compound**	**Eg (eV)**	**Reference**		**S. No**	**Name of the Compound**	**Eg (eV)**	**Reference**
1	ZnS	3.6	[26]		7	ZnS	3.78	[33]
	$Zn_{0.9}Pb_{0.1}S$	3.5				$Zn_{1-x}Co_xS$ (x=0.1)	3.81	
	$Zn_{0.8}Pb_{0.2}S$	3.3				$Zn_{1-x}Co_xS$ (x=0.2)	3.85	
	$Zn_{0.7}Pb_{0.3}S$	3.0				$Zn_{1-x}Co_xS$ (x=0.3)	3.93	
	$Zn_{0.6}$Pb0.4S	2.9			8	ZnS	3.92	[44]
2	Bulk ZnS	3.68	[41]			$Cu_{0.02}Zn_{0.98}S$	3.88	
	ZnS NP undoped	4.43				$Cu_{0.04}Zn_{0.96}S$	3.85	
	Ni (1.2%) - ZnS	4.35				$Cu_{0.06}Zn_{0.94}S$	3.76	
	Ni (2.5%) - ZnS	4.34				$Cu_{0.08}Zn_{0.92}S$	3.67	
	Ni (5.0%) - ZnS	4.28				$Cu_{0.1}Zn_{0.9}S$	3.51	
3	ZnS	3.92	[30]		9	ZnS	3.92	[45]
	Fe - ZnS	3.8				$Co_{0.04}Zn_{0.96}S$	3.76	
	Ni - ZnS	3.64				$Co_{0.06}Zn_{0.94}S$	3.69	
	C0 - ZnS	3.49				$Co_{0.08}Zn_{0.92}S$	3.67	
4	$Cd_{0.8}$ $Zn_{0.2}S$	2.55	[46]			$Co_{0.10}Zn_{0.9}S$	3.62	
	$Cd_{0.7}Pb_{0.1}$ $Zn_{0.2}S$	3.16			10	$Cd_{0.8}Zn_{0.2}S$	2.58	[19]

	$Cd_{0.4}Pb_{0.4}Zn_{0.2}S$	3.48				$Cd_{0.8}Zn_{0.2}S$: $Na_{0.03}$	2.80	
	$Cd_{0.2}Pb_{0.6}Zn_{0.2}S$	4.37				$Cd_{0.8}Zn_{0.2}S$: $Na_{0.1}$	2.70	
	$Cd_{0.1}Pb_{0.7}Zn_{0.2}S$	4.40				$Cd_{0.8}Zn_{0.2}S$: $Na_{0.2}$	2.83	
	$Pb_{0.8}Zn_{0.2}S$	4.43				$Cd_{0.8}Zn_{0.2}S$: $Na_{0.3}$	3.18	
5	$Cd_{0.9}Zn_{0.1}S$ (Cu=0)	3.79	[43]		11	$Cd_{0.8}Zn_{0.2}S$	2.52	[20]
	$Cd_{0.9}Zn_{0.1}S$(Cu=2%)	4.01				$Cd_{0.8}Zn_{0.2}S$: $Sm_{0.01}$	3.18	
	$Cd_{0.9}Zn_{0.1}S$(Cu=4%)	3.96				$Cd_{0.8}Zn_{0.2}S$: $Sm_{0.02}$	3.08	
	$Cd_{0.9}Zn_{0.1}S$(Cu=6%)	3.69				$Cd_{0.8}Zn_{0.2}S$: $Sm_{0.03}$	3.01	
6	ZnS	3.82	[31]					
	3.30% Ni -ZnS	3.70				$Cd_{0.8}Zn_{0.2}S$: $Sm_{0.04}$	2.87	
	5.36% Ni – ZnS	3.67				$Cd_{0.8}Zn_{0.2}S$: $Sm_{0.05}$	2.82	

V. CONCLUSION

The bandgap values strongly depend upon the crystal structure of the material. Consequently, it depends on the synthesis conditions and the synthesis process. From the above analysis, it is found that energy bandgap of ternary semiconductor compounds varie from 0.6eV to 3.6eV, based on doping and the host material. Bandgap of 1.6eV is optimally desired for solar cell applications to have maximum efficiency. Thus, by virtue of larger band gap, the present reviewed ternary materials come under a very much suitable category for window materials in solar applications. Therefore, they are the suitable materials for fabrication of electroluminescent devices and solid-state solar window layers.

Increasing bandgap lowers the conductivity of the semiconductor. So, these materials are not suitable for wide bandgap applications directly. Rare earth elements favour the electrical conductivity of the semiconductor compound so that study of rare earth dopants may be taken as future work on these ternary compounds.

Conflict-of-Interest Statement: The authors have no conflicts of interest to declare. All co-authors have seen and agreed with the contents of the manuscript and there is no financial interest to report. We certify that the submission is original work and is not under review at any other publication.

REFERENCES

[1] Green M A 2009 *Prog. Photovoltaic: Res. Appl.* **17** 183
[2] Jin C Q, Zhong W, Zhang X, Deng Y, Au C T and Du Y N 2009 *Cryst. Growth Des.* **9** 4602
[3] Azizi S, Dizaji H R and Ehsani M H 2016 *Optik.* **127** 7104
[4] Ziabari A A and hodsi F E G 2013 *Mater. Sci. Semicond. Process.* **16** 1629
[5] Vasudeva Reddy Y, Kumar T M, Shekharam T and Nagabhushanam M 2019 *Chem. Phys. Lett.* **715** 147
[6] Chaku A K, Singh P K and Bhaskar Bhattacharya 2017 *J. Mater. Sci. Mater. Electron.* **28** 11163
[7] Abza T, Ampong F K, Hone F G, Nkum R K and Boakye F 2018 *Thin Solid Films.* **666** 28
[8] Ampong F K, AM Awudza J, Nkum RK, Boakye F, Thomas PJ and Paul O'Brien 2015 *Solid State Sci.* **40** 50
[9] Raji P, Ramachandran K and Sanjeeviraja C 2006 *J Mater Sci.* **41** 5907
[10] Shi J, Yan H, Wang X, Feng Z, Lei Z and Li C 2008 *Solid State Commun.* **146** 249
[11] Tahab S M, Omran A H and Saleh S M 2014 *Sci. Semicond. Process.* **26** 49
[12] Ravishankar S and Balu A R 2016 *Surface Engi.* **33** 506
[13] Touati B, Gassoumi A, Alfaify S and Tuski N K 2015 *Mat.Sci.Semi.Process.* **34** 82
[14] Veena E, Kasturi V and Shivakumar G K 2017 *optik.* **144** 528
[15] Vasudeva Reddy Y, Mohan kumar T, Shekharam T and Nagabhushanam M 2018 *Solid State Sci.* **82** 29
[16] Adeoye A E, Ajenifuja E, Alayande S O, Ogunmola E D, Adeyemi O A and Fasasi A F 2020 *SN Appl. Sci.* **2** 1560
[17] Fang X, Zhai T, Gautam U K, Li L, Wu L, Bando Y *et al* 2011 *Prog. Mat. Sci.* **56** 175
[18] H.M, Hennayaka M N and Lee H S 2013 *Thin solid films.* **548** 86
[19] Yellaiah G, Hadasa K and Nagabhushanam M 2013 *J. Alloys Compd.* **581** 805
[20] Yellaiah G, Hadasa K and Nagabhushanam M 2014 *J. Cryst. Growth.* **386** 62
[21] Yellaiah G, Shekharam T, Hadasa K and Nagabhushanam M 2014 *J. Alloys Compd.* **609** 192
[22] Yellaiah G and Nagabhushanam M 2015 *J. Cryst. Growth* **421** 33
[23] Hadasa K, Yellaiah G and Nagabhushanam M 2014 *J. Mater. Sci.* **37** 53
[24] Hadasa K, Yellaiah G and Nagabhushanam M 2014 *Optik.* **125** 6602
[25] Vijaya T, Ram Mohan Rao S, Nagabhushanam M, Srinu Naik S and Rajam B 2016 *Int. J. Eng. Res. Technol.* **5** 362

[26] Y. Vasudeva Reddy, T. Mohan Kumar, T. Shekharam, M. Nagabhushanam 2018 *Solid State Sciences* **82** 29
[27] Jothibasa M, Manoharanb C, Johnson Jeyakumara S, Praveen P, Kartharinal Punithavathya I and Prince Richard J 2018 *Sol Energy.* **159** 434
[28] Sunil Kumar and Verma N K 2015 *J. Supercond. Nov. Magn*. **28** 137
[29] Amaranatha Reddy D, Liu C, Vijayalakshmi R P and Reddy B K 2013 *J. Alloys Compd*. **582** 257
[30] Dehghani Z, Shadrokh Z and Nadafan M 2017 *Optik*. **131** 925
[31] Sanjeev Kumar R, Veeravazhuthi V, Muthukumarasamy N, Thambidurai M and Vishnu Shankar D 2015 *Superlattices Microstruct*. **86** 552
[32] Talwatkar S S, Sunatkari A L, Tamgadge Y S, Pahurkar V G and Muley G G 2014 *Appl. Phys A.* **118** 675
[33] Sambasivam S, Paul Joseph D, Lin J G and Venkateswaran C 2009 *J. Solid State Chem.* **182** 2598
[34] Kaur P, Kumar S, Singh A, Chen C L, Dong C L, Chan T S *et al* 2015 *Superlattices Microstruct*. **83** 785
[35] Amaranatha Reddy D, Murali G, Vijayalakshmi R P, Reddy B K, and Sreedhar B 2011 *Cryst. Res. Technol*. **46** 731
[36] Srinivasa Rao B, Rajesh Kumar B, Rajagopal Reddy V and Subba Rao T 2011 *Chalcogenide Lett.* **8** 46
[37] Devi L S, Devi K N, Sharm B I and Sarma H N 2014 *Indian J Phys*. **88** 477
[38] Thambidurai M, Muthukumarasamy N, Dhayalan, Velauthapillai, Murugan N, Jharna Chaudhuri *et al* 2012 *J. Mater. Sci. Mater. Electron.* **23** 618
[39] Shekharam T, John Siddarth G, Vasudev Reddy Y and Nagabhushanam M 2018 *J. Lumin.* **197** 56
[40] Amaranatha Reddy D, Murali G, Vijayalakshmi R P, Reddy B K, and Sreedhar B 2011 *Cryst. Res. Technol.* **46** 731
[41] Namrata Dixit, Nishant Anasane, Mukesh Chavda, Dhananjay Bodas and Hemant P. Soni 2013 *Mater. Res. Bull.* **48** 2259
[42] Amaranatha Reddy D, Sambasivam S, Murali G, Poornaprakash B, Vijayalakshmi R P, Aparna Y *et al* 2012 *J. Alloys Compd.* **537** 208
[43] Devadoss I and Muthu Kumaran S *2015 Physica E Low Dimens. Syst. Nanostruct.* **72** 111.
[44] Laxminarasimha Rao V, Shekharama T and Nagabhushanam M 2013 *IOSR j. appl. phys.* **3** 27
[45] Laxmi Narasimha Rao V, Shekharam T, Hadasa K, Yellaiah G and Nagabhushanam M 2013 *IOSR j. appl. phys.* **5** 19.